

Has the Recent Global Warming Caused Increased Drying over Land?

Aiguo Dai*, Taotao Qian, and Kevin E. Trenberth
National Center for Atmospheric Research (NCAR)[§], Boulder, CO

Abstract

To assess potential changes in surface moisture conditions over global land from 1948 to 2002 associated with surface warming, the Palmer Drought Severity Index (PDSI) and land surface model-simulated soil water content were analyzed. The PDSI was derived using observed precipitation and temperature and a simple land surface model (Dai et al. 2004), while the model simulations were done by running the Community Land Model (CLM), a comprehensive land surface model designed for climate simulations, in an offline mode using observation-based precipitation, surface air temperature, radiation and other atmospheric forcing. The precipitation and temperature forcing data were derived by combining 6-hourly synoptic variations in the NCEP/NCAR reanalysis with monthly data derived from station records, while observed cloudiness and the ISCCP-based satellite solar radiation data were used to adjust the year-to-year variations and mean biases in the reanalysis surface downward solar radiation. Both the PDSI and CLM-simulated soil water content show a large drying trend over northern hemispheric land since the middle 1950s, with widespread drying over much of Eurasia, northern Africa, Canada and Alaska. In the Southern Hemisphere, the land surface was wet in the 1970s and relatively dry in the 1960s and 1990s; and there was a large drying trend from 1974 to 1998 although trends over the entire 1948-2002 period are small. Decreases in land precipitation in recent decades are main cause for the drying trends, although large surface warming during the last 2-3 decades also contributed to the drying significantly.

1. Introduction

Most climate models predict increased drying over inland areas due to enhanced evaporation associated with increased surface temperatures (e.g., Robock et al. 2004). Surface air temperatures over global land areas have increased sharply since the late 1970s. Has this warming caused any drying trends over global land areas?

Historical records of soil moisture content are available only for a few regions and often are very short in length (Robock et al. 2000). A rare, 45-yr record of soil moisture over Ukraine agricultural lands show little change over the last 3 decades (Robock et al. 2004).

In order to assess the potential drying associated with surface warming, Dai et al. (2004) used the Palmer Drought Severity Index (PDSI) as a proxy of surface moisture conditions. The PDSI is correlated with available top-1m soil moisture data, and it co-varies closely with observed streamflow when integrated over large river basins. Dai et al. (2004) found that the global

very dry areas, defined as $PDSI < -3.0$, have more than doubled since the 1970s, with a large jump in the early 1980s due to an ENSO-induced precipitation decrease and subsequent expansion primarily due to surface warming; while global very wet areas ($PDSI > +3.0$) declined slightly during the 1980s. Together, the global land areas in either very dry or very wet conditions have increased from ~20% to 38% since 1972, with surface warming as the primary cause after the middle 1980s. These results point to increased risk of droughts as anthropogenic global warming progresses.

Here we further examine the potential changes in surface moisture conditions through analyses of data and model-simulated fields. To supplement observational data, we used a comprehensive land surface model, namely the Community Land Model (CLM3.0) (Bonan et al. 2002; Dai et al. 2003), to simulate global land surface conditions with realistic atmospheric forcing for the period 1948-2002. For our purpose, the long-term trends in the forcing data (precipitation, surface temperature and solar radiation, etc.) need to be as realistic as possible. We therefore devoted considerable efforts to create the historical forcing data for driving the CLM.

2. Data and model simulations

* Corresponding author address: Aiguo Dai, NCAR/CGD,
P.O.Box 3000, Boulder, CO 80307.

§ The National Center for Atmospheric Research is sponsored by the National Science Foundation.

Table 1 lists the data sets used in this study. The forcing data for driving the CLM were derived by adjusting the monthly mean of the NCEP/NCAR reanalysis temperature and precipitation data to observed monthly data: $P = P_{mo} / P_{mr} * P_r$, where P_{mo} observed monthly precipitation from Chen et al. (2002), P_{mr} is monthly precipitation from the reanalysis, P_r is 6 hourly precipitation from the reanalysis. The same was done for surface air temperature, where the Climate Research Unit (CRU) temperature data set (Jones and Moberg 2003) was used. Fig. 1 shows that the reanalysis surface air temperature is about 1°C cooler than observed and the reanalysis precipitation has discontinuities around 1965 in the Northern Hemisphere and around 1972 in the Southern Hemisphere.

For surface downward solar radiation, the monthly time series are strongly correlated with cloud amount in the reanalysis. However, the reanalysis cloud amount averaged over global land has a spurious downward trend that caused an upward trend in the reanalysis solar radiation. Because of this, we used the observed cloud amount from the CRU (New et al. 2002; Mitchell et al. 2004) to adjust the monthly time series of reanalysis radiation data based on the cloud-radiation regression relationship in the reanalysis. These adjusted radiation data were further corrected for mean biases using the satellite-based estimates of global surface radiation fluxes (Zhang et al. 2004) by comparing their mean over a common period (1983-2001). We found that the cloud-adjusted radiation co-varies more closely than the original reanalysis radiation with observed downward solar radiation from the Global Energy Balance Archive (GEBA) database (Gilgen et al. 1998) (Fig. 2).

We did not directly use the satellite data because they have much larger year-to-year variations than the cloud-adjusted reanalysis radiation. The GEBA data are available only for limited locations and often have a short record length; hence we used them only for validation purpose.

Forcing data of 10-m wind speed and surface specific humidity were directly interpolated from the NCEP/NCAR reanalysis 6-hourly data, as these fields have smaller effects on land surface conditions than precipitation, temperature and radiation, and also because there are no observational data sets for these fields readily available to us. The surface temperature and humidity were interpolated to a 10m level (required by the CLM) using a scheme described in Large and Pond (1982). The 6-hourly data were linearly interpolated to 3-hourly resolution and onto T42 (~2.8° x 2.8°) and 0.5° grids on which the CLM was run.

The CLM is a comprehensive land surface model designed to be used in coupled climate system models (Bonan et al. 2002; Dai et al. 2003). It has fairly sophisticated treatment of the soil (up to 3.5 m depth), vegetation, photosynthesis, surface fluxes, runoff and river routines. Dai et al. 2003; Oleson et al. 2004). Here we ran the CLM in an offline mode forced with specified atmospheric forcing. The CLM was run several hundreds of years using recycled forcing data to get stable water content in the deep soil layers, and the last 55 years (1948-2002) of the simulation were analyzed. We ran the CLM on both 0.5° and T42 (~2.8°) grids, the results are similar on regional and large-scales. We use the T42 simulation here.

TABLE 1. Data sets used in this study. All are monthly except stated otherwise.

Variables	Type & coverage	Resolution	Period	Source & Reference
Precipitation, P	rain-gauge, land	2.5°x 2.5°	1850-2003	Dai et al. 1997; Chen et al. 2002
Temperature, T	surface obs., land	5° x 5°	1851-2003	CRUTEM2, Jones & Moberg 2003
Streamflow	station, land		1-100+ yrs	NCAR, Dai & Trenberth 2002
Soil moisture	station, land		10-21 yrs	Robock et al. 2000
	Illinois, USA	19 stations	1981-2001	Hollinger & Isard 1994
	China	43 stations	1981-1991	Robock et al. 2000
	Mongolia	42 stations	1978-1993	Robock et al. 2000
	former USSR	50 stations	1972-1985	Vinnikov & Yeserkepova 1991
Cloud Cover	sfc. obs., land	0.5°x 0.5°	1901-2000	CRT_TS_2.02 (New et al. 2002)
PDSI	derived, land	2.5°x 2.5°	1870-2003	Dai et al. (2004)
Surface solar radiation	satellite, global	2.5°x 2.5°	1983-2001	NASA GISS, Zhang et al. (2004)
	station, land	~95 stations	1960-1990	GEBA, Gilgen et al. (1998)
Sfc. T, q, wind speed, Ps, solar radiation, P	reanalysis, global	~1.9°x 1.9°	1948-2002	NCEP/NCAR, Kalnay et al. (1996)
		6-hourly		

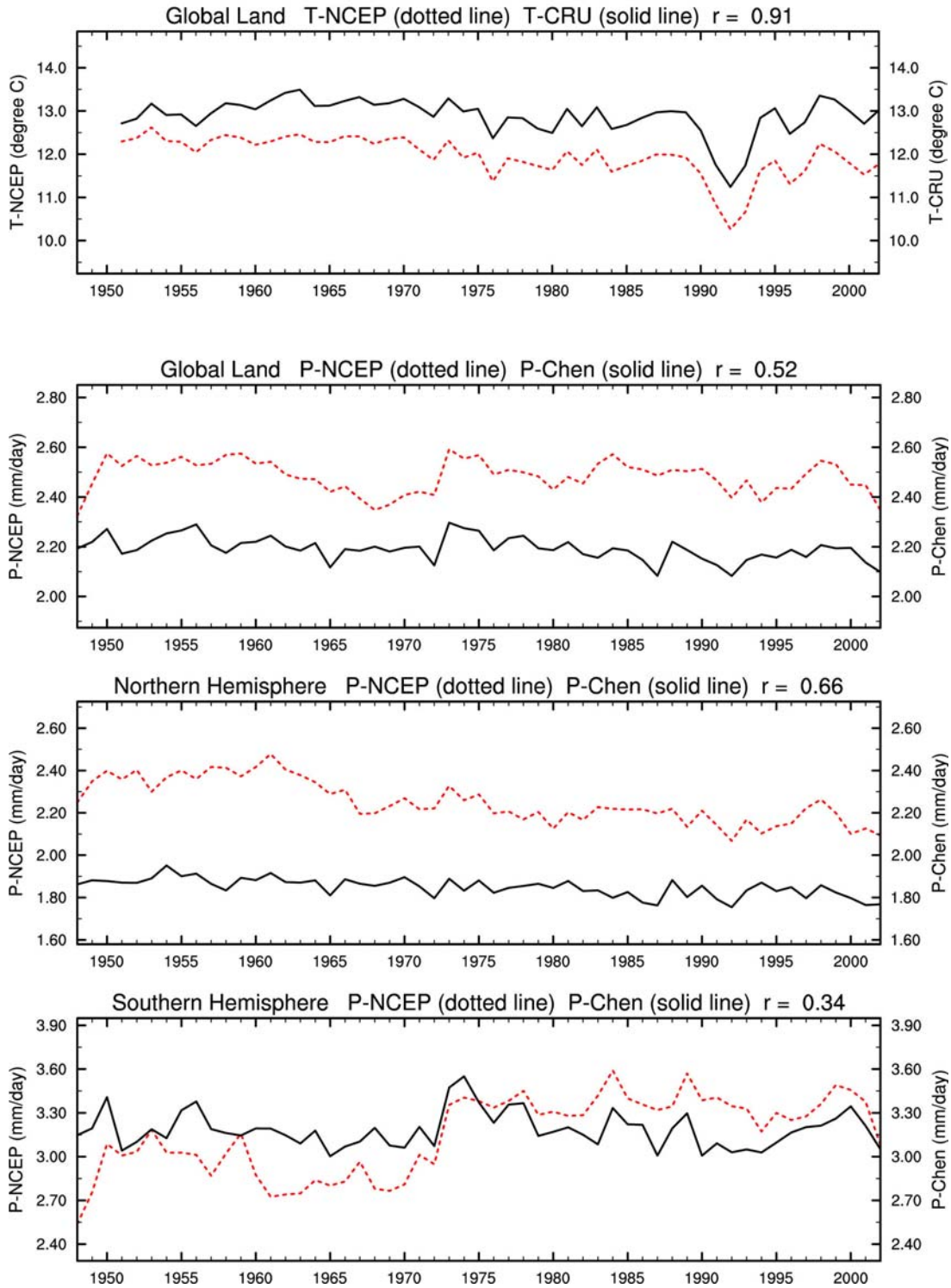


Fig. 1: Time series of annual surface air temperature (top) and precipitation (lower 3 panels) averaged over global (60°S-75°N) and hemispheric (for precipitation only) land areas from the NCEP/NCAR reanalysis (dotted line) and station data (solid line: precipitation from Chen et al. 2002; temperature from Jones and Moberg 2003).

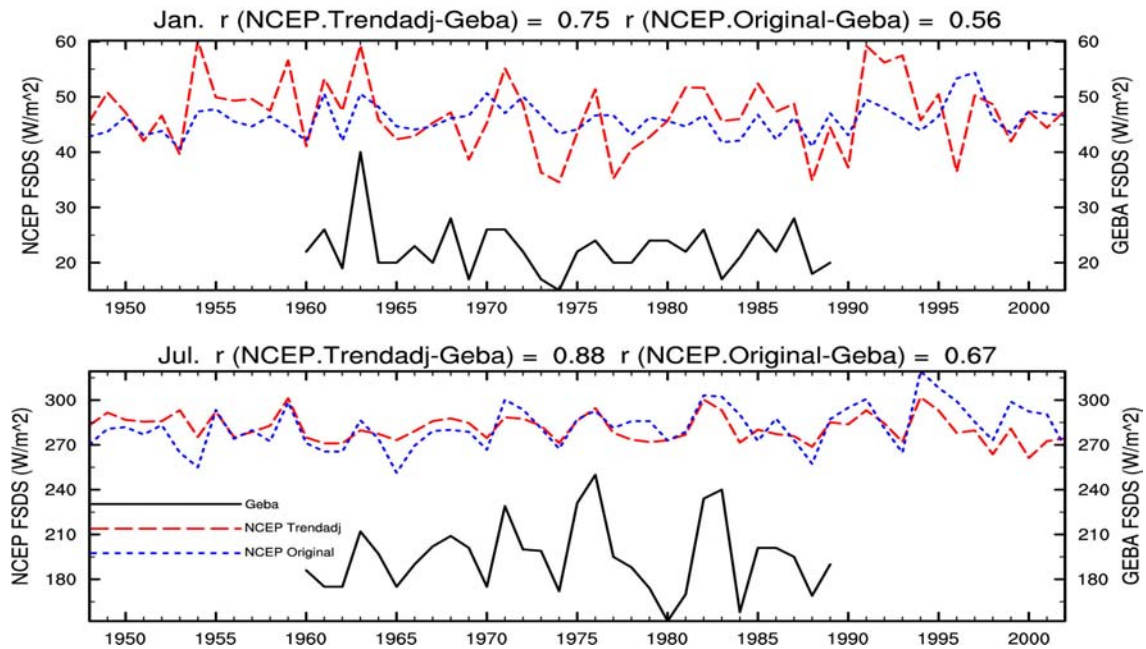


Fig. 2: Comparison of January (top) and July (bottom) surface downward solar radiation at a GEBA station (9.38°E, 54.28°N) from observations (solid line), the NCEP reanalysis (short-dashed line), and the cloud-adjusted reanalysis radiation (long-dashed line). Also shown on the top of the panels are correlation coefficients (from left to right) between the observed and cloud-adjusted radiation and between the observed and reanalysis radiation.

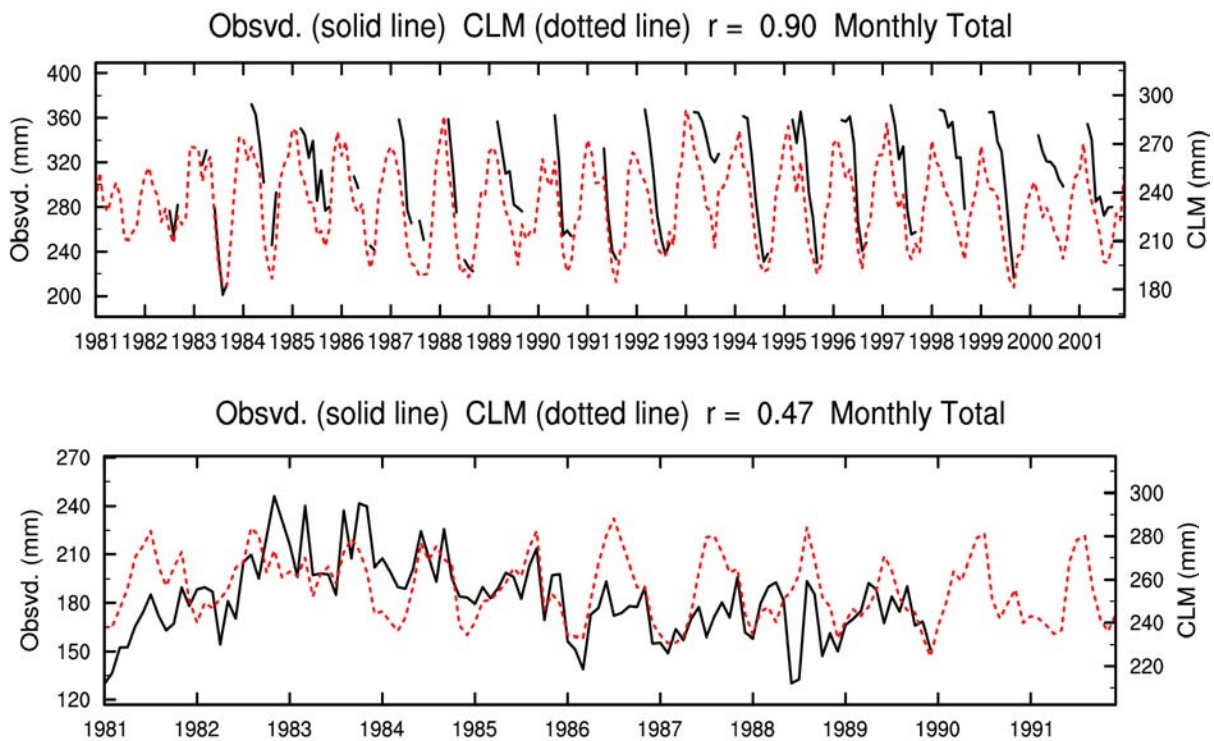


Fig. 3: Monthly Time series of observed (solid) and CLM-simulated (dashed) top-1m soil moisture content over southern Illinois (top) and South China (bottom). The correlation coefficient (r) between the two curves is shown on the top.

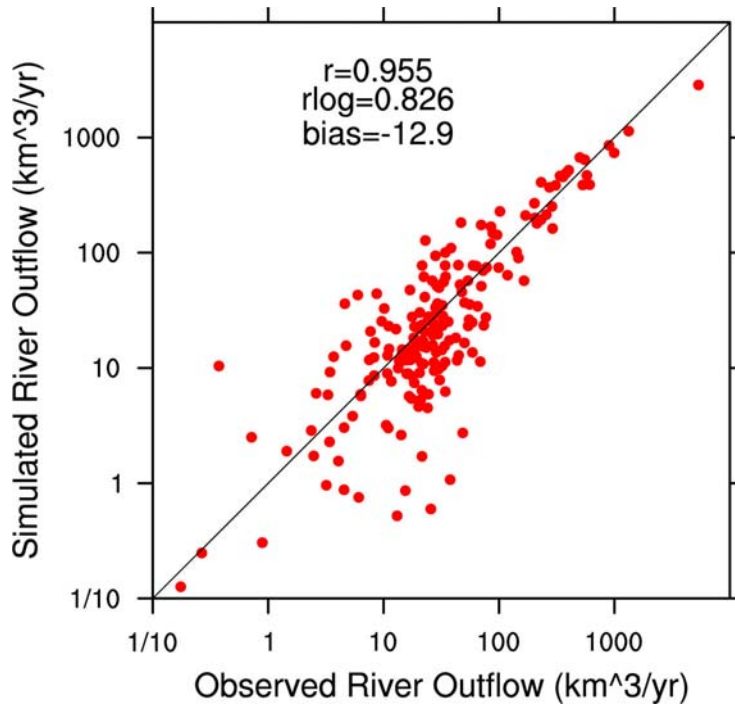


Fig. 4. Scatter-plot of observed and CLM-simulated long-term mean annual river outflow rates for world's top 200 rivers. The observations are from Dai and Trenberth (2002). The linear (r), logarithmic (r_{log}) correlation coefficients and the mean (simulated minus observed) bias are shown.

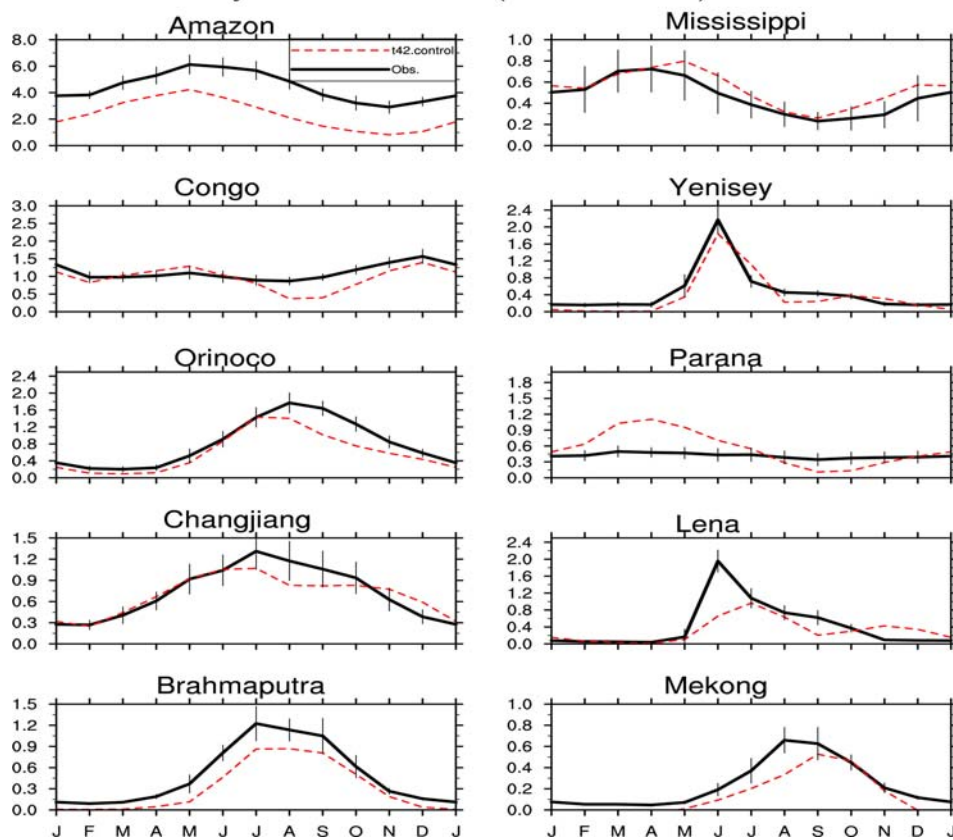


Fig. 5. CLM-simulated (Mean annual cycle of river outflow rates ($10^2 \text{ km}^3/\text{mon}$)) for world's largest ten rivers.

The CLM simulations were validated using available soil moisture and streamflow data. Fig. 3 shows that the CLM captures the observed soil moisture variations reasonably well over southern Illinois and South China, although large mean biases exist. The CLM-simulated river outflow rates are also comparable to observed for most of world's major rivers (Fig. 4). The annual cycle of river outflow rates for world's ten largest rivers are also captured by the CLM, although the CLM consistently underestimates Amazon's outflow in both offline and coupled simulations.

3. Changes in Surface Moisture Conditions

Fig. 6 compares the global and hemispheric mean PDSI (from Dai et al. 2004) and the CLM-simulated top-1m soil water (including both liquid and solid phases) anomalies during 1948-2002. The PDSI considers accumulated effects of past moisture demand (i.e., evaporation) and supply (i.e., precipitation), and it seems to have a slightly longer memory than the simulated soil water. Otherwise, the two are strongly correlated, especially in the Southern Hemisphere.

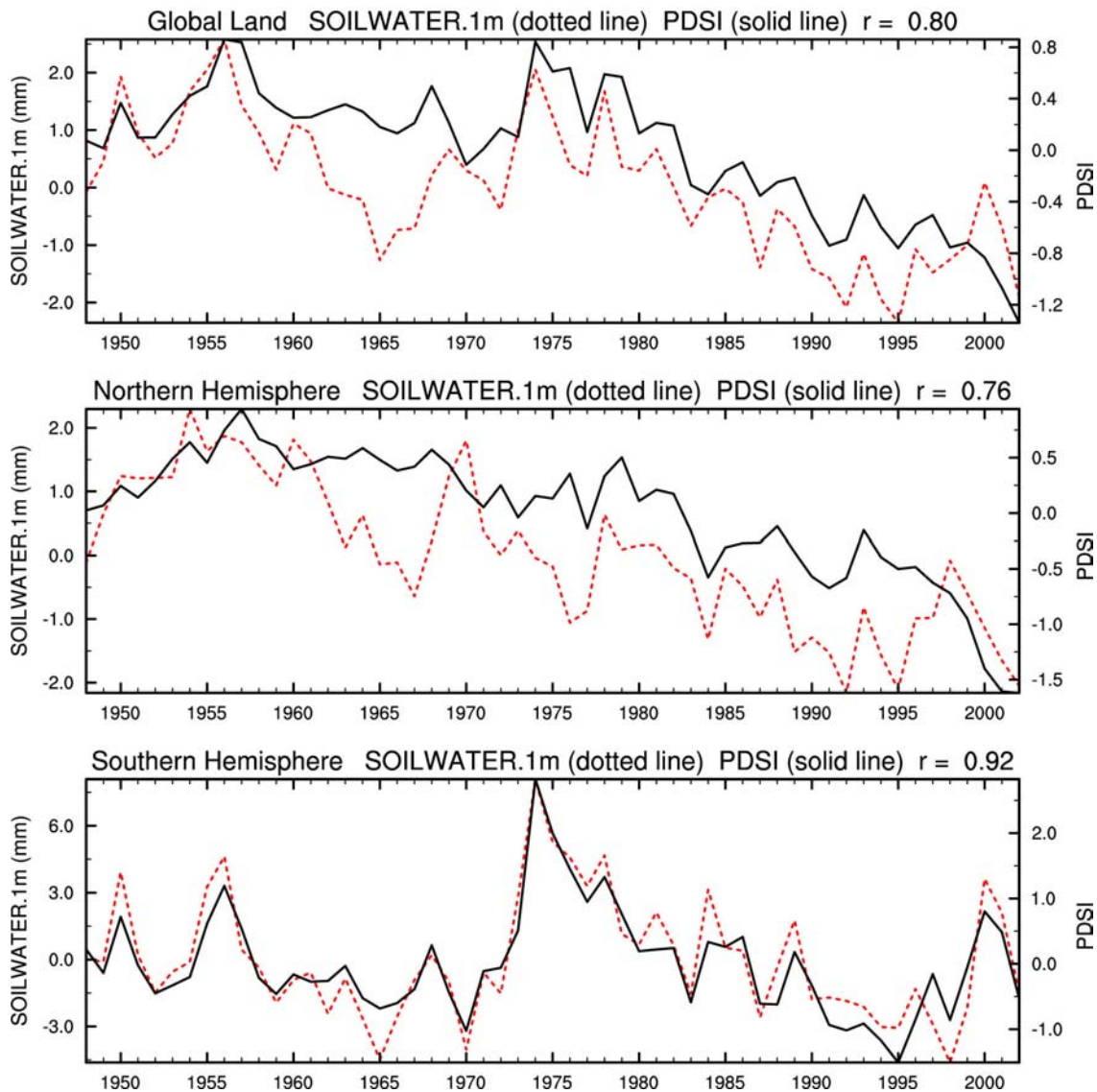


Fig. 6. Anomalies of top-1m soil water content (dotted line, mm) simulated by the CLM and the PDSI (solid line, from Dai et al. 2004) averaged over global (60°S-75°N) (top), Northern Hemisphere (middle), and Southern Hemisphere (bottom) land areas.

Both the PDSI and the simulated soil water content show a steady drying trend in the Northern Hemisphere since the middle 1950s (Fig. 6). The magnitude of the drying is very large considering that a PDSI of -1.0 may be considered as drought conditions. In the Southern Hemisphere, the land surface was relatively wet in the 1970s and dry during the 1960s and 1990s; and the drying from 1974 to 1998 is substantial although trends over the entire period are small.

Fig. 7 shows the spatial distribution of linear trends

in the PDSI and the CLM-simulated top-1m soil water content during 1948-2002. The patterns of the two maps are significantly correlated ($r=0.42$), although regional differences exist (e.g., over northern Africa and northern Europe). Widespread drying over Eurasia, Canada and Alaska, western (including the Sahel) and southern Africa, and eastern Australia is suggested by both the PDIS and the soil water, while much of the United States, Argentina and western Australia has become wetter during 1940-2002 (Fig. 7).

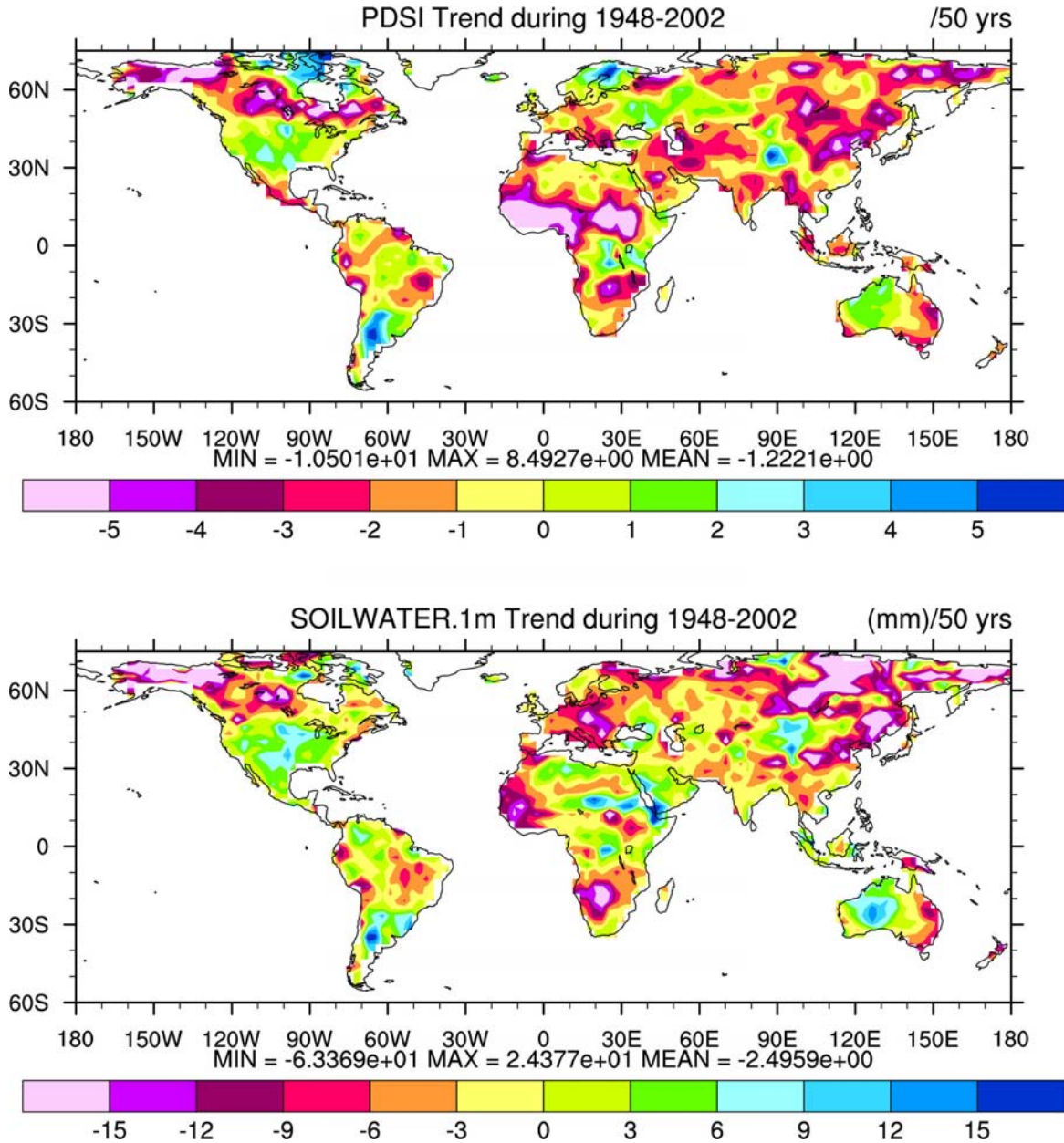


Fig. 7. Distributions of the linear trends in annual PDSI (top, change/50 yrs, from Dai et al. 2004) and CLM-simulated top-1m soil water (bottom, mm/50 yrs).

Defining very dry and very wet areas as those with $PDSI < -3.0$ and $PDSI > +3.0$, respectively, Fig. 8 shows that the very dry area has more than doubled (from ~12% to 30%) since the 1970s, with a large jump in the early 1980s due to precipitation decreases and subsequent expansion primarily due to surface warming. The precipitation decreases around the early 1980s occurred mainly over ENSO-sensitive regions such as the Sahel, southern Africa and East Asia as El Niños, which reduce rainfall over these, became more prominent after the late 1970s. In contrast, the warming-induced drying has occurred over most land areas, with the largest effects in northern mid- and high-latitudes (Dai et al. 2004). Coinciding with increases in the very dry areas from the early 1980s to early 1990s, the global very wet land areas declined by ~5%, with precipitation as the major contributor during the early 1980s and temperature more important thereafter. Together, the

global areas under either very dry or very wet conditions decreased slightly by ~7% from 1950 to 1972, with precipitation as the primary contributor. Since 1972, the dry plus wet percentage areas have increased from ~20% to 38% (a 90% increase), with surface warming as the primary cause after the middle 1980s (Fig. 9).

Fig. 9 shows that the CLM-simulated global soil water is significantly correlated with both precipitation and surface air temperature. The decreasing precipitation and increasing temperature from the early 1970s to early 1990s work together to produce a steady drying trend in global land during this period. Global land precipitation has increased since the late 1990s. Global soil water has responded to this precipitation change but in a delayed (because of soils' memory) and muted manner (because of increased evaporation due to increased warming).

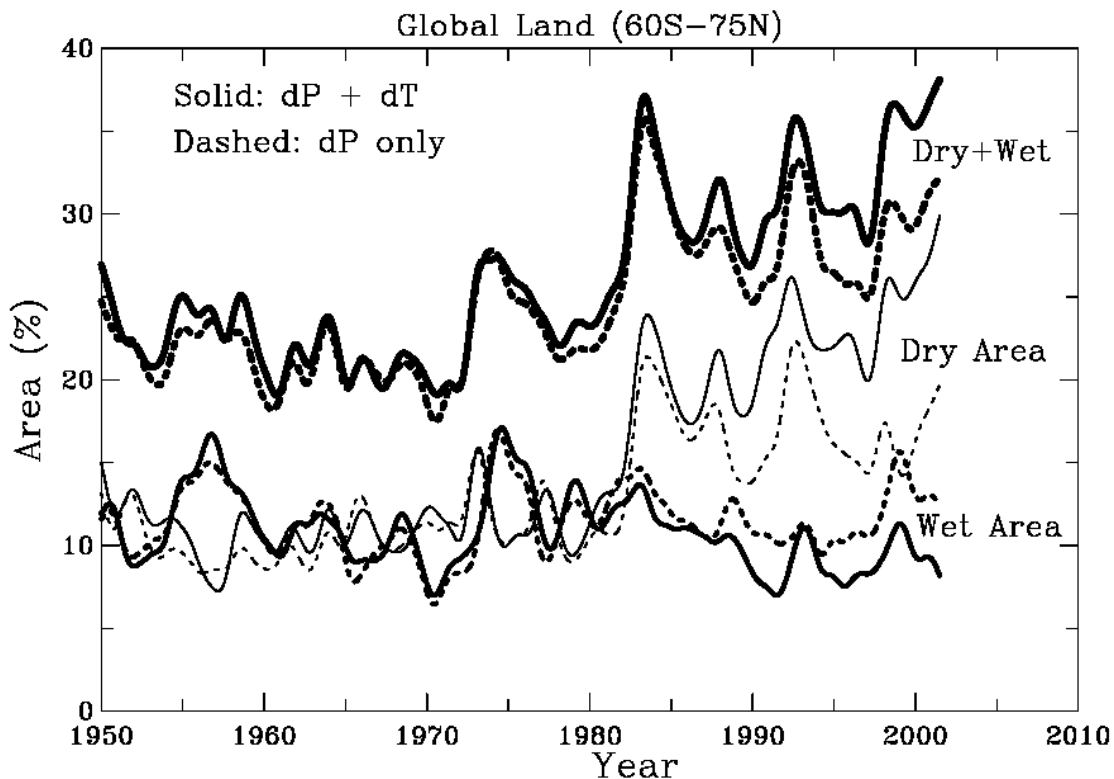


Fig. 8: Smoothed time series of the percentage of the total land areas within 60°S-75°N that were in very dry ($PDSI < -3.0$, thin lines), very wet ($PDSI > +3.0$, medium lines), and very dry or wet (thickest lines at the top) conditions from 1950 to 2002. The solid lines are based on the PDSI calculated with both precipitation and temperature changes while the dashed lines are without temperature changes (i.e., due to precipitation alone). (From Dai et al. 2004)

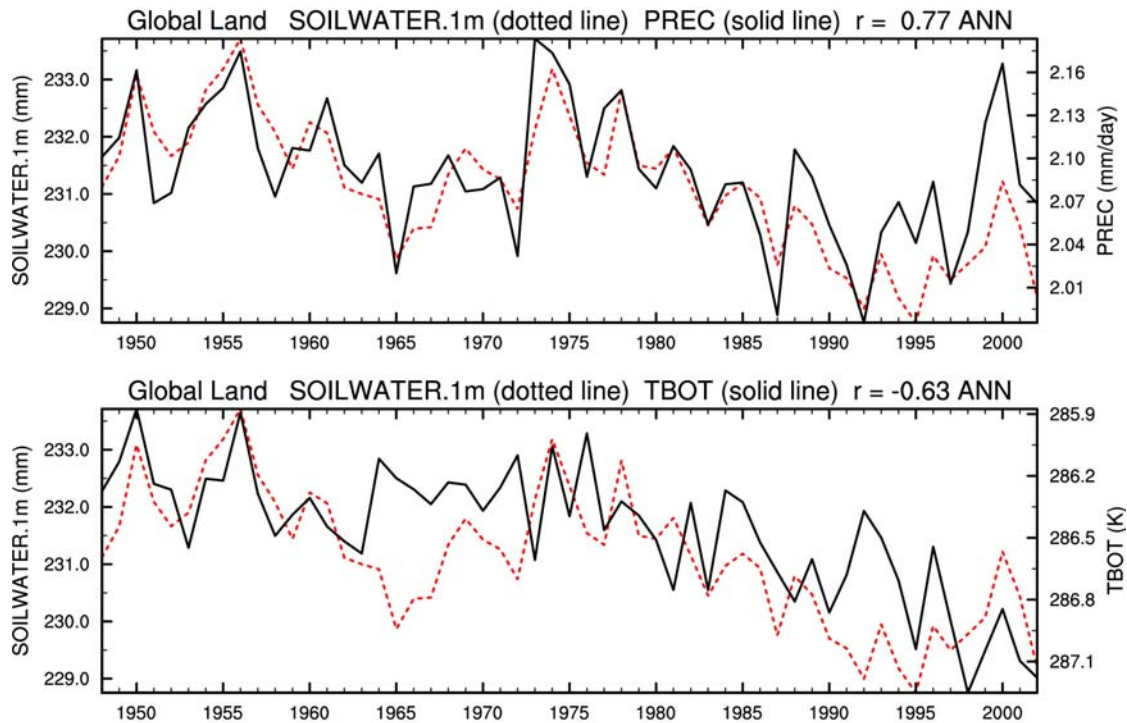


Fig. 9. CLM-simulated global land top-1m soil water content (dashed line) compared with global land precipitation (top panel, solid line) and temperature (bottom, solid line, scales increase downward on the right side).

4. Summary

To assess potential changes in surface moisture conditions over global land from 1948 to 2002, the PDSI and CLM-simulated soil water content were analyzed. The PDSI was derived using observed precipitation and temperature and a simple land surface model (Dai et al. 2004), while the CLM simulations were done by running the CLM, a comprehensive land surface model, in an offline mode using observation-based precipitation, surface air temperature, radiation and other atmospheric forcing. The precipitation and temperature forcing data were derived by combining 6-hourly synoptic variations in the NCEP/NCAR reanalysis with monthly data derived from station records, while observed cloudiness and the ISCCP-based satellite solar radiation data were used to adjust the year-to-year variations and mean biases in the reanalysis surface downward solar radiation.

Both the PDSI and CLM-simulated soil water content show a large drying trend over northern

hemispheric land since the middle 1950s, with widespread drying over much of Eurasia, northern Africa, Canada and Alaska. In the Southern Hemisphere, land surface was wet in the 1970s and dry during the 1960s and 1990s; and there was a large drying trend from 1974 to 1998 although trends over the entire 1948-2002 period are small.

Decreases in land precipitation in recent decades are main cause for the drying trends, although large surface warming during the last 2-3 decades also contributed to the drying significantly.

Acknowledgments: We thank Gordon Bonan, Keith Oleson, Sam Levis, Steve Yeager and Mariana Vertenstein for assistant with the CLM and forcing data, and Y.-C. Zhang and Beate Liepert for providing the satellite and GEBA radiation data, respectively. This research was supported by NSF Grant No. ATM-0233568 and NCAR's Water Cycle Across Scales Initiative. The PDSI data set can be downloaded from <http://www.cgd.ucar.edu/cas/catalog/climind/pdsi.html>.

References

- Bonan, G. B., K. W. Oleson, M. Vertenstein, S. Levis, X. Zeng, Y. Dai, R. E. Dickinson, and Z. Yang, 2002: The Land Surface Climatology of the Community Land Model Coupled to the NCAR Community Climate Model. *Journal of Climate*, **15**, 3123-3149.
- Chen, M., P. Xie, J. E. Janowiak, and P. A. Arkin, 2002: Global land precipitation: a 50-yr monthly analysis based on gauge observations. *J. Hydrometeorol.*, **3**, 249-266.
- Dai, A. G. and K. E. Trenberth, 2002: Estimates of freshwater discharge from continents: Latitudinal and seasonal variations. *J. Hydrometeorol.*, **3**, 660-687.
- Dai, A., K. E. Trenberth, and T. Qian, 2004: A global data set of Palmer Drought Severity Index for 1870-2002: Relationship with soil moisture and effects of surface warming. *J. Hydrometeorology*, in press.
- Dai, Y. J., X. B. Zeng, R. E. Dickinson, I. Baker, G. B. Bonan, M. G. Bosilovich, A. S. Denning, P. A. Dirmeyer, P. R. Houser, G. Y. Niu, K. W. Oleson, C. A. Schlosser, and Z. L. Yang, 2003: The Common Land Model. *Bull. Amer. Meteorol. Soc.*, **84**, 1013-1023.
- Gilgen, H., M. Wild, and A. Ohmura, 1998: Means and trends of shortwave irradiance at the surface estimated from global energy balance archive data. *Journal of Climate*, **11**, 2042-2061.
- Hollinger, S. E., and S. A. Isard, 1994: A soil moisture climatology of Illinois. *J. Climate*, **7**, 822-833.
- Jones, P. D. and A. Moberg, 2003: Hemispheric and large-scale surface air temperature variations: An extensive revision and an update to 2001. *J. Climate*, **16**, 206-223.
- Kalnay, E., M. Kanamitsu, R. Kistler, W. Collins, D. Deaven, L. Gandin, M. Iredell, S. Saha, G. White, J. Woollen, Y. Zhu, M. Chelliah, W. Ebisuzaki, W. Higgins, J. Janowiak, K. C. Mo, C. Ropelewski, J. Wang, A. Leetmaa, R. Reynolds, R. Jenne, and D. Joseph, 1996: The NCEP/NCAR 40-year reanalysis project. *Bulletin of the American Meteorological Society*, **77**, 437-471.
- Large, W. G., and S. Pond, 1982: Sensible and latent heat flux measurements over the ocean. *J. Phys. Oceanogr.*, **12**, 464-482.
- Mitchell, T.D., Carter, T.R., Jones, P.D., Hulme, M., New, M., 2004: A comprehensive set of high-resolution grids of monthly climate for Europe and the globe: the observed record (1901-2000) and 16 scenarios (2001-2100). *Journal of Climate*, submitted.
- Robock, A., K. Y. Vinnikov, G. Srinivasan, J. K. Entin, S. E. Hollinger, N. A. Speranskaya, S. Liu, and A. Namkhai, 2000: The global soil moisture data bank. *Bull. Amer. Meteorol. Soc.*, **81**, 1281-1299.
- Robock, A., M. Mu, K. Vinnikov, I. V. Trofimova, and T. I. Adamenko, 2004: Fifty five years of observed soil moisture in Ukraine: No summer desiccation (Yet). *Geophys. Res. Lett.*, submitted.
- Vinnikov, K. and I. B. Yeserkepova, 1991: Soil moisture: empirical data and model results. *Journal of Climate*, **4**, 66-79.
- Zhang, Y-C., W.B. Rossow, A.A. Lacis, V. Oinas and M.I. Mishchenko, 2004, Calculation of radiative fluxes from the surface to top-of-atmosphere based on ISCCP and other global datasets: Refinements of the radiative transfer model and the input data, *J. Geophys. Res.*, in press.